

Photocatalytic reduction of CO₂ into solar fuels using M-BTC metal organic frameworks for environmental protection and energy applications

P. Thamizhazhagan^{a,*}, P. Sivakarthik^b, J. Balaji^c

^a*Department of Electrical and Electronics Engineering, University College of Engineering, Panruti, Tamilnadu, India 607106*

^b*Department of Chemistry, University College of Engineering, Panruti, Tamilnadu, India 607106*

^c*Department of Physics, University College of Engineering, Panruti, Tamilnadu, India 607106*

The photo catalytic reduction of CO₂ into solar fuels and value-added chemicals is very interesting in the view point of green chemistry. It offers a clean and energy saving solution for the major environmental challenges of global warming and climate change. Recently, the use of transition metal-based MOFs photocatalyst has become more popular in this process due to their porous structure, abundance of metal site and organic functionalities. Herein, we derived divalent transition metal-based MOFs (Zn²⁺, Cu²⁺, Mn²⁺) as photocatalyst materials. The obtained photo catalyst materials were characterized by XRD, XPS, SEM and TEM technique to know the structural, optical, photocatalytic and morphological properties. They were subsequently tested for photo catalytic reduction of CO₂ and results shows that all the heterostructure M-BTC possess significant ability of photo catalytic reduction of CO₂. Moreover, among the three catalyst, Zn-BTC MOFs showed the outstanding performance towards of photo catalytic reduction of CO₂. Gas chromatographic analysis confirms the formation of value-added products such as CH₃OH, Methane and Carbon Monoxide. The possible photo catalytic mechanism discussed and supported its outstanding performance.

(Received June 10, 2021; Accepted October 11, 2021)

Keywords: Metal organic frameworks, Benzene tricarboxylic acid, Photo catalytic reduction, CO₂ absorption, Value added products

1. Introduction

Provision of sufficient energy to everyone has become biggest challenge for the entire world caused by continuously growing global energy demands. Global energy demands have been growing exponentially due to population explosion, industrialization, growing economy and urbanization. In most of the countries, traditional energy resources like coal, oil, gas have contributed significantly to meet the energy demands. Fossils fuels are world's primary energy source, comprise 80 per cent of current global energy demand consequently energy systems of most countries based on fossil fuels [1,2]. On the other hand, combustion of fossil fuels for the production of energy can yield serious of problems such as accelerating global warming, diminishing air quality standard and harms to human health [3]. The use of fossil fuels is main responsible for most dangerous environmental problem's climate change and global warming. As we burn fossil fuels, the concentration of CO₂ in the atmosphere is increasing on year which enhances the natural greenhouse effect and warms the planet. For protecting society and environment from the risk of global warming and climate change, it is important to reduce the accumulation of CO₂ in atmosphere which has prompted research on converting CO₂ into most valuable products [4-6], researchers make special efforts to convert CO₂ into more useful compounds.

* Corresponding author: thamizh@ucep.edu.in

Photocatalytic reduction of CO₂ is a promising technique since it uses readily and permanently available solar light to convert main greenhouse gases into more valuable products such as carbon monoxide [7-10], methanol [11,12], formic acid [13,14] and methane [15,16]. Up to now various photocatalyst such as semiconductors, polymers, carbon-based materials etc have been developed for the photocatalytic reduction of CO₂ and to increase the efficiency of the catalyst [17-21]. In the photocatalytic conversion of CO₂ into value added product, catalyst play a vital role and it should absorb light and activate CO₂ simultaneously.

In recent years enormous efforts have been focussed towards the development of new class of metal organic frameworks (MOFs) by linking multi dentate organic ligands with metal or metal clusters. Due to their porosity and high surface volume ratio, they have emerged as promising materials for various applications such as catalysis [22,23], photocatalysis [24-26], drug delivery [27-29], redox reactions [30-32]. Among the various applications, MOFs with photocatalysis features have received great deal of interest to explore its novel applications as well as due to their tailored specific properties [33]. Literature review reported that MOFs have large CO₂ absorption ability at only at high pressure and its activity is not comparable to that of inorganic semiconductors. Improving CO₂ absorption capacity at low pressure and enhancing its activity comparable to that of semiconductor is a scientific challenge [34].

To overcome this challenge many attempts have been made such as metal doping [35], functionalization with alkyl amine group [36,37], making empty unsaturated metal coordination sites [38,39]. Among them doping impurities on MOFs have been paid more attention; noble metal-based MOFs [40], Ag based functionalized MOFs [41], Au based MOFs [42], Pt based MOFs [43] have proved their better performance towards the photocatalytic reduction of CO₂. Moreover, doping of transition metals [44,45] such as Co, Ni, Fe, Cu on MOFs for high photocatalytic activity as well as selective reactivity still challenge and the research efforts have been attracting towards the development of non-noble metal-based MOFs due to its cost effectivity [46,47], high performance and durability [48-50].

In this work, we synthesized divalent transition metal ion based (Zn²⁺, Cu²⁺, Mn²⁺) MOFs using BTC by facile hydrothermal route. And for the first time, the photocatalytic absorption of CO₂ by as synthesized M-BTC MOFs has been investigated. The excellent photocatalytic reduction of CO₂ is attributed for Zn-BTC MOFs compared to that of other Cu-BTC and Mn-BTC MOFs. The possible mechanism and reusability of the catalyst have been evaluated and discussed in detail.

2. Experimental Procedure

2.1. Materials

Zinc nitrate, Manganese nitrate, Copper nitrate, ethanol, Benzene tri carboxylic acid, DMF were purchased from Sigma Aldrich, India. All the chemicals were in high purity AR grade and hence used without further purification. For the preparation of solutions double distilled water was used.

2.2. Synthesis of Zn-BTC MOF

Zn-BTC MOF was synthesized by hydrothermal method based on the Literature [51,52]. The schematic synthetic procedure is given in Fig.1. In a typical synthesis, mixture of 3 mmol of (2.5 g) Zinc nitrate and 3 mmol of (1.1 g) 1,3,5 BTC were mixed with equal volume of ethanol and dimethyl formamide and made up to 100 ml. The resulting mixture kept in an ultra-sonication bath for 5 minutes. Then it was transferred to Teflon lined stainless steel auto clave and it was heated to 150 °C for 10 hours. Then it was exposed to atmosphere for gradual cooling at room temperature. After cooling, the formed crystals were separated and washed thrice with hot ethanol for complete purification and removal of dimethyl formamide and dried well in room temperature. The resulting product is named as Zn-BTC MOF or Zn-MOF.

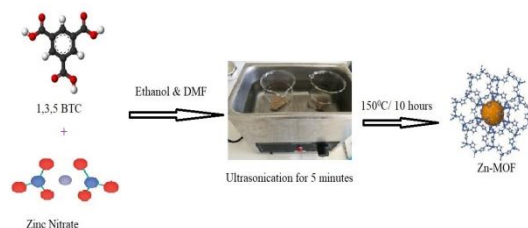


Fig.1. Schematic diagram of synthesis of Zn-MOF.

2.3. Synthesis of Cu-BTC and Mn-BTC MOFs

For the synthesis of Cu-BTC and Mn-BTCMOFs, the same synthetic procedure and experimental conditions were followed. 3 mmol of $\text{Mn}(\text{NO}_3)_2$ and 3 mmol of $\text{Cu}(\text{NO}_3)_2$ were used to introduce the metal ion in MOF. The resulting product is named as Mn-BTC(Mn-MOF) and Cu-BTC(Cu-MOF) respectively.

2.4. Photocatalytic CO_2 reduction experiments

The simple schematic diagram of photo catalytic reduction experiment shown in Fig.2. Photocatalytic reduction of CO_2 was carried out using double wall cylindrical quartz reactor with capacity of 250 ml and it was connected to the closely fitted cylindrical tube. The reactor was water jacketed for maintaining the temperature. 10 mg of synthesized photo catalyst was dispersed in 100 ml dd water under ultrasonication bath for the formation of suspension and added into the photo reactor. Right before the irradiation, the reaction mixture was bubbled with CO_2 gas for 1 hour in order to saturate the solution. After purging of CO_2 , the solution was irradiated with mercury lamp equipped with 320-500 nm filter. The resulting products were analyzed using calibrated GC technique for every one hour for the total reaction time of 9 hour. Blank experiments were also conducted without catalyst and irradiation in order to confirm the formation of products only due to the photo catalytic reaction. The various factors influenced to rate of photochemical reactions such as irradiation time, concentration of CO_2 , pH, catalyst loading also studied through various experiments. Each experiment was repeated for twice in order to get replication.

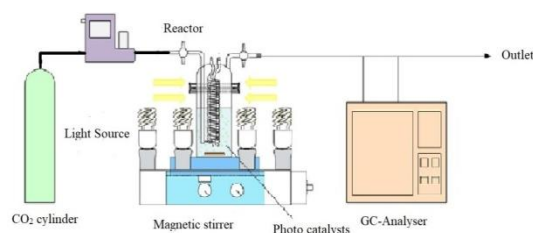


Fig.2. Schematic diagram of photocatalytic reduction experiment.

3. Results and Discussion

3.1. Characterization of synthesized Zn-BTC, Cu-BTC and Mn-BTC MOFs

With the support of Bruker D8 diffractometer using $\text{Cu-K}\alpha$ radiation ($\lambda=1.5418 \text{ \AA}$) in the 2-theta range 10 to 80 degree, synthesized all metal doped MOFs were characterized for identification of crystallinity of the samples. The recorded XRD pattern of the samples are shown in Fig.3. Diffraction pattern of all the samples shows clear and sharp peaks and it confirms the good crystallinity of all the catalysts. All the diffraction peaks match well with standard pattern confirms the successful formation of all MOFs. All the main characteristic peak observed for Zn-MOF indexed to hexagonal crystalline structure for it according to review of literature [53,54]. The XRD pattern of Mn-MOFs and Cu-MOFs illustrates that it is available in monoclinic phase

and all the peaks are well matched [55,56]. No peak shift or additional peaks observed for all the sample compared to standard illustrates that high purity and crystallinity of all the catalysts.

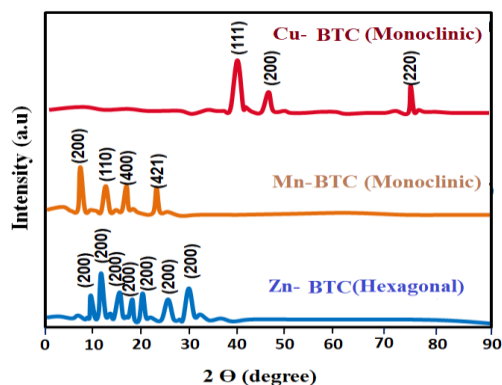


Fig.3. XRD pattern of Zn-BTC, Mn-BTC and Cu-BTC.

3.2. SEM and TEM Analysis

Scanning Electron Microscopic and Transmission Electron Microscopic images of the photo catalyst were recorded and are depicted in Fig. 4.

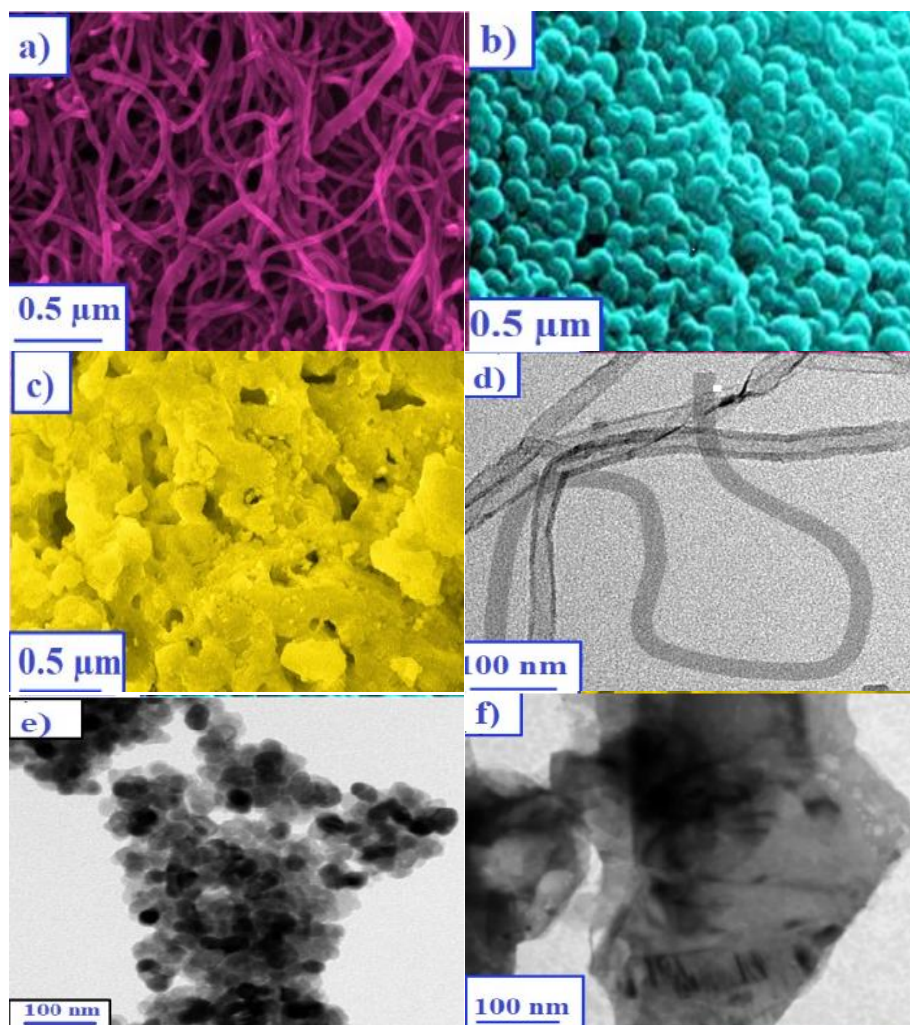


Fig.4. SEM images of (a) Zn-BTC (b) Mn-BTC (c) Cu-BTC TEM images of (d) Zn-BTC (e) Mn-BTC (f) Cu-BTC.

In Fig.4, a, b & c shows the SEM photographs of respective M-BTC MOFs. High quality crystals and very good shape shown in images suggesting that all the catalysts are in high crystallinity and this report consistent with already reported XRD data. It also reveals that different morphology observed for different metals but homogeneous morphology for individual species. Zn metal gives nanotube like structure and also the morphology changed into sheet like structure for Mn and ball like structure for Cu metals. Fig.4 d, e, f shows TEM images of the samples. From the TEM picture it was noticed that Zn-BTC exhibit as tubes with diameter of 20 nm and length is around 200 -300 nm whereas wrinkle type sheets with the diameter range of 150 nm for Mn-BTC. It can also be observed that Cu-BTCnanoparticles are well dispersed throughout its structure and spherical nanoparticles with average diameter about 30-40 nm. Further the elemental mapping depicted in Fig.3. g, h,i&j confirms the presence of Zn, Mn, Cu and N and uniform distribution of all.

3.3. BET Analysis

For effective photocatalytic activity, the materials with high surface area can facilitate the catalytic reactions which develops the activity of the catalysts. To demonstrate the specific surface area of as synthesized catalyst and porous structure, N_2 adsorption-desorption isotherm analysis performed and depicted in Fig.5. a. All the catalysts exhibit type IV N_2 adsorption-desorption isotherm and sharp increase of isotherm at low p/p_0 and uniform hysteresis loop at the large range, which is between 0.7 to 0.9 reflecting nearness of mesoporous structure [57]. The BET surface area of the samples calculated as 101.2 m^2/g , 86.2 m^2/g and 66.1 m^2/g for Zn-BTC, Mn-BTC and Cu-BTC respectively. The results indicates that Zn-MOF have large surface are, which may be expected for high catalytical activity. The identical pore size distribution curve shown in Fig.5. b. and pore diameter value were calculated as 12.2, 21.4 and 30.8 respectively.

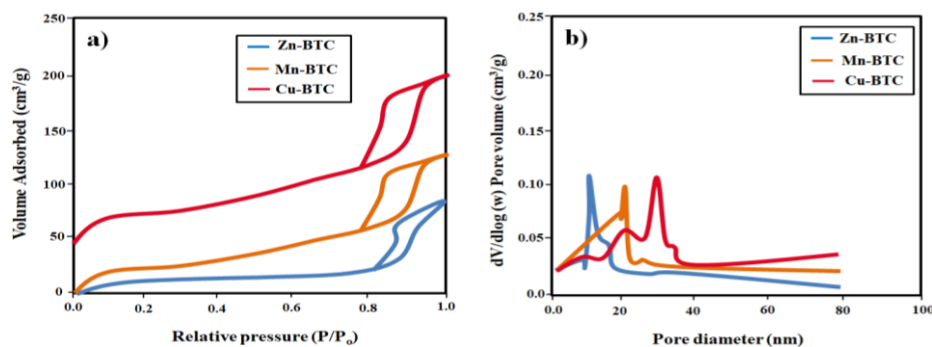


Fig.5. (a) N_2 adsorption and desorption analysis and (b) corresponding pore size distribution of Zn-BTC, Mn-BTC, Cu-BTC.

3.4. XPS Analysis

To explore the internal structure and chemical states of elements, XPS characterization of Zn-BTC, Mn-BTC and Cu-BTC performed and the results are shown in Fig.6. a. As shown in figure a wide survey scan of the samples shows only the presence of Zn, Mn, Cu in the respective MOFs without any additional elements as impurities in the sample. In Zn-BTC, the high-resolution spectra of Zn (Fig.6.b), there are two peaks with BE values 1015.1 eV and 1024.2 eV which can be assigned for $p_{1/2}$ type and $p_{3/2}$ type of orbital of 2p zinc respectively. Similarly, in Mn-BTC, the high-resolution spectra of Mn (Fig.6.c), there are two peaks with BE values 650.1 and 642.2 eV corresponds to the $p_{3/2}$ and $p_{1/2}$ type of 2p orbital of Mn. Furthermore, in Cu-BTC (Fig.6.d), Cu 2p scanning shows two unsymmetrical peaks at 943.8 and 960.8 eV which are attributed to $p_{3/2}$ and $p_{1/2}$ type of 2p orbital of Cu.

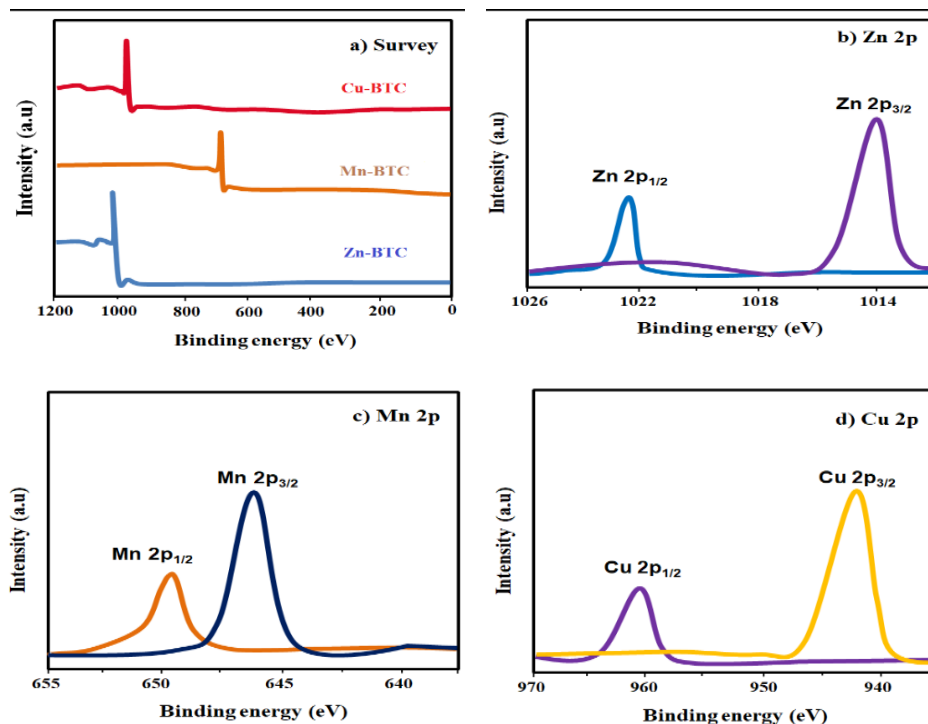


Fig.6. (a) XPS spectra of Zn-BTC, Mn-BTC and Cu-BTC; High resolution spectra of (b) Zn-2p; (c) Mn-2p; (d) Cu-2p.

3.5. Evaluation of photocatalytic reduction of CO₂

Photo catalytic activity of as prepared MOFs catalyst examined by photoreduction of CO₂ molecules under light irradiation for 9 hours. At first, to confirm the reduction of CO₂ results from light mediated photo catalytic reaction, series of controlled blank experiments carried out by without catalysts or light irradiation or CO₂. The results reveals that the reaction did not occur in all the three cases and it confirms the photo catalytic activity of as prepared catalysts as well as thermally mediation process is not possible for CO₂ reaction. Photo generated electron is the primary cause for the photocatalytic activity of the catalysts. To confirm it, transient photo current-time experiment was carried out and the photo current – time plot obtained by repeating light on and off cycle, depicted in Fig.7. It was indicated that all the catalyst generates photo current when light is on and disappear when light is off. It reveals that all the catalysts are sensitive to light irradiation and generates the electron during the photo physical process. As compared to Mn-MOF and Cu-MOF, Zn-MOF showed larger photocurrent due to its structure.

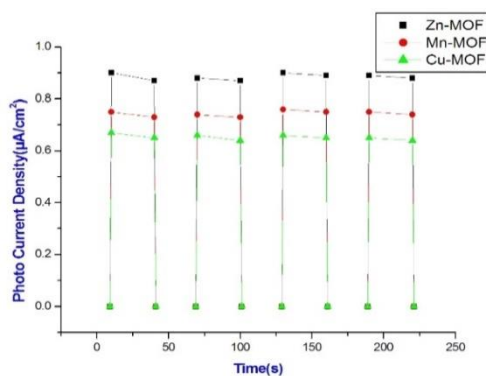


Fig.7. Photo current-time plot of Zn-BTC, Mn-BTC and Cu-BTC.

Time required for the complete photo reduction of CO₂ for different catalyst investigated with help of IR spectroscopy by comparing CO absorption peak. It was noted for one hour time interval up to 6 hours. The complete disappearance of absorption intensity of CO took place only after 8 hours for all the catalyst. So, the remaining investigation carried out up to 9 hours. The CO reduction percentage under different time interval given in Fig. 8. and it indicates the maximum conversion takes place between 4-5 hours.

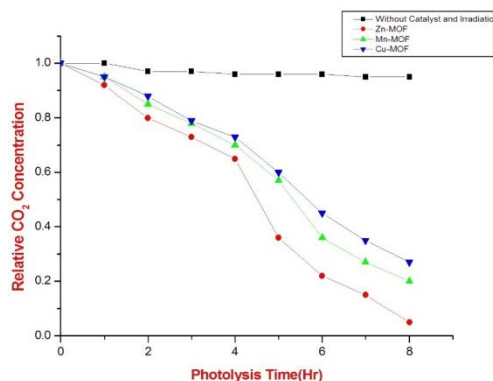


Fig.8. CO₂ reduction by photocatalyst under different time interval.

Afterwards, ability photocatalytic absorption of CO₂ for as synthesized MOFs catalysts investigated under light illumination and reported that all the samples were effective towards the reduction reaction and CH₄, CO, H₂ and CH₃OH are obtained as products. Methane and hydrogen are formed as major whereas trace amount of carbon monoxide and methanol are formed. As soon as illuminating the Zn-MOF catalysts with radiation of 320-500 nm, we observe 66 ppm g⁻¹ h⁻¹ of methane, 17.8 ppm g⁻¹ h⁻¹ of methanol and 2.3 ppm g⁻¹ h⁻¹ of hydrogen and less than 1 ppm of carbon monoxide. The production of various products by different catalysts under different time intervals are given in Table 1 and plotted in Fig.9. All the catalyst gives high percentage of methane compared to other products.

Table 1. Evaluation of yield of CH₄ and CH₃OH by photocatalytic reduction of CO₂ by different catalyst under different time interval.

	Yield of CH ₄ (ppmg ⁻¹ h ⁻¹)			Yield of CH ₃ OH (ppmg ⁻¹ h ⁻¹)		
	Zn-MOF	Mn-MOF	Cu-MOF	Zn-MOF	Mn-MOF	Cu-MOF
1	66	54	50	2.3	1.9	1.8
2	76	65	60	3.3	2.2	2.2
3	88	70	65	4.6	2.4	2.2
4	102	88	75	5.8	3.2	3.1
5	122	96	90	6.9	4.0	3.8
6	126	102	95	7.3	5.2	5.0
7	129	113	100	7.9	6.2	6.0
8	132	117	107	8.2	6.5	6.6

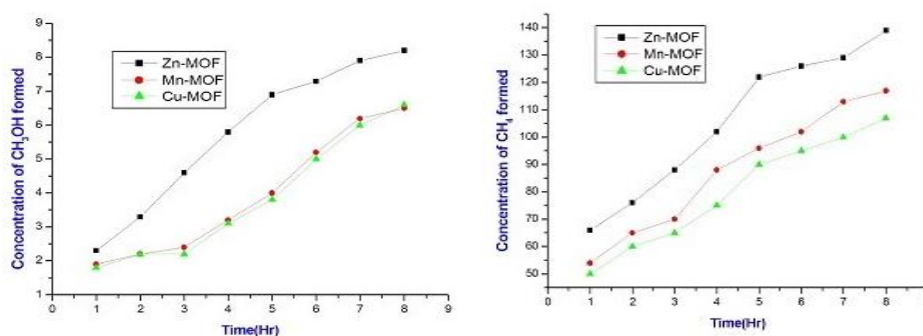


Fig.9. Photocatalytic formation of CH₃OH and CH₄ under different time interval.

In addition, some comparative experiments carried out to find the more suitable catalyst for production of methanol and the results are given in Fig. 10. It is a clear evidence that Zn-MOF is the superior catalytic activity for photocatalytic removal of CO₂ as well as production of methanol.

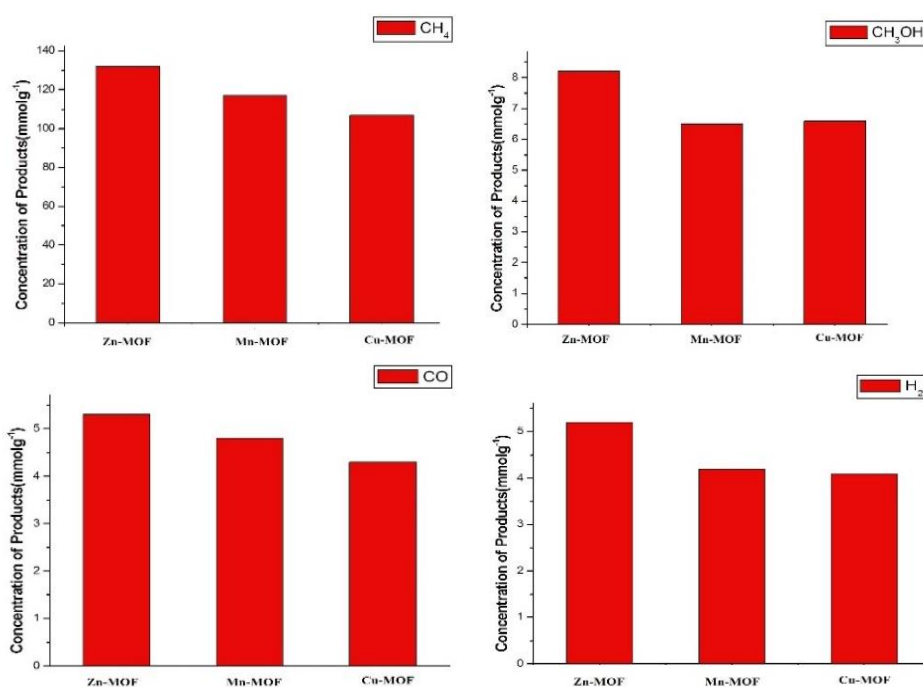


Fig.10. Evaluation of yield of (a) CH₄ (b) CH₃OH (c) CO (d) H₂ by photocatalytic reduction of as synthesized catalysts.

3.6. Effect of catalyst dosage

To examine the effect of catalyst concentration on the reduction of carbon dioxide into methanol, different catalyst ratios were tested from 1% by weight to 5% by weight and their reports are given in Fig. 11. It clearly showed initially the increase of catalyst concentration increases the product and after attaining its saturation point it decreases the catalytic activity. In this study 3% by weight is its optimum loading ratio and gives maximum yields. It is also revealing that the increase of yield is not exactly proportional to its loading ratio. Initially increasing the catalyst concentration causes for increasing active sites and surface area for adsorption of gaseous molecules due to increasing the number of electrons caused for the photocatalytic reaction. After attaining its optimum level, decreasing activity due to turbidity of the suspension which reduces the penetration of light. [58,59].

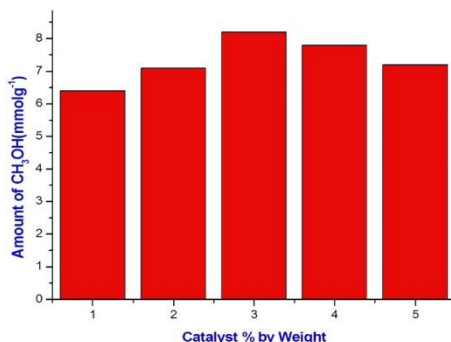


Fig.11. Effect of catalyst concentration on production of CH₃OH by photocatalytic reduction of Zn-MOF.

3.7. Effect of pH

The effect of pH on the production of methanol was also explored in this work and shown in Fig. 12. The results show the pH also play on important role in the production of methanol toward the photocatalytic reduction of CO₂. At very low pH, nearly 1-2 range pH the amount of product is slightly lower than higher acidic value while at basic pH diminishing the rate of methanol production. This is due to the surface charge of the catalyst was influenced by pH. The surface charge is positive at acidic pH and hence promotes the conversion by rapid adsorption of negative charged species. But the surface charge is negative at basic pH and hence retard the adsorption of negative charged species.

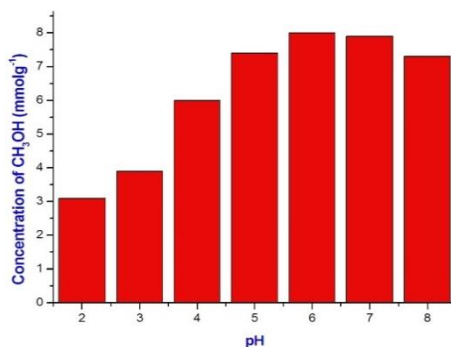


Fig.12. Effect of pH on production of CH₃OH by photocatalytic reduction of Zn-MOF.

3.8. Reusability of the catalyst

Furthermore, to understand the regeneration ability and stability of the catalyst upon reuse, 3% by weight of Zn-MOF irradiated with visible light for 8 hr at ambient temperature and pH6.3 were chosen because they would be favourable for the formation maximum yield of methanol. When compared to the previously obtained results, there is no change in the yield of methanol up to 10 runs. Almost constant amount of product obtained for successive runs. The catalytic efficiency of catalyst used in each cycle was calculated by comparing it with previous result and the reports are plotted as efficiency versus number of cycles (Fig.13). It clearly conveys that the catalyst can be reused without obvious lost in its activity and also suggest that there is no loss in its activity up to five runs and it lost its activity in slightly only after fifth runs which may be due to loss of some surface area due to agglomeration and sintering of nanoparticles during the process.

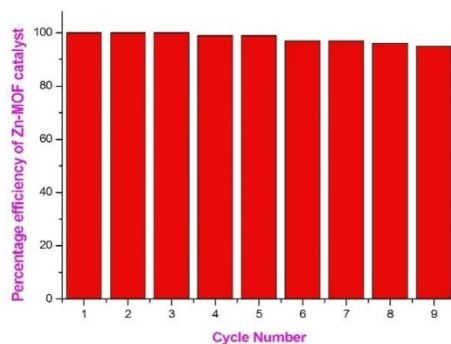


Fig.13. Reusability test of the catalyst.

3.9. Mechanism of photocatalytic reduction of CO₂

Finally, the mechanism of photocatalytic reduction of CO₂ is studied and shown in Fig.14. When Zn-MOF excited via visible light irradiation, electron(e⁻) – hole(h⁺) pair is formed on the surface of the catalyst. So, the formation of electron-hole pair on MOF is the initial process and serve as site for photo oxidation and reduction process. The excited hole reacted with adsorbed water molecules on the surface of catalyst to produce the hydroxy radicals (OH[·]) and H⁺ ions and further oxidised by hydroxy radicals to produce O₂ and H⁺ species [60]. Hydrogen radical is also formed from proton by interaction with electron. The catalytic conversion of CO₂ takes place through gain of these electrons. Since photocatalytic absorption of CO₂ is multi electron transfer reaction, based on the number of electrons transferred various products such as methanol, formic acid, carbon monoxide, ethanol, ethane, methane may be formed. Mechanism of formation of methanol from CO₂ given in Fig.15.



Fig.14. Mechanism of photo catalytic reduction of CO₂ by Zn-MOF.

In addition, the order of photo catalytic efficiency for reduction of CO₂ is found as Zn-MOFs > Mn-MOF > Cu-MOF. Among the three catalysts, Zn-MOFs performs as superior catalyst towards the photocatalytic reduction ability of CO₂. This may be related to its structure and size. The modification of MOF using Zn reducing the band gap energy greater compared to Mn and Cu and hence increases the photo catalytic activity [61]. In general, the reduction of CO₂ by photo catalytic reaction depends on two important factors such as the capability of catalyst to absorb CO₂ and efficiency of electron transfer [62]. Since CO₂ absorption ability is related to surface charge and area, smaller size well as nano tube like orientation accelerates the photo catalytic activity of Zn-MOF. Also, Zn promote the interparticle charge migration and facilitate photo generated electron transfer from conduction band to valence band more compared to Mn and Cu.

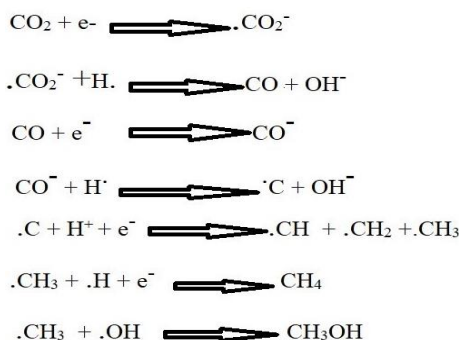


Fig.15. Mechanism of formation of CH_3OH from CO_2 by photo catalytic reduction.

4. Conclusion

Zn-MOF, Mn-MOF and Cu-MOF were successfully synthesized by hydrothermal method. Tubular, sheet and spherical morphology observed for Zn, Mn, and Cu-MOF respectively. The photo catalytic activity of the catalyst studied towards absorption of CO_2 . Transition metal doped MOF showed catalytical activity towards the reduction of CO_2 and produce methane and methanol as product. Zn-MOF showed better performance compared to other and produce maximum yields.

Superior performance of Zn-MOF due to its morphology and smaller size. Zn-MOF maintain its catalytical activity up to several runs. This work present transition metal doped MOF having strong ability to absorb CO_2 , which may have excellent photo catalytic activity towards the photo reduction of CO_2 . Zn-MOF may be used for promising applications in CO_2 photo reductions and for environmental applications such as control the global warming and climate change.

References

- [1] Y.Sugiawani, S.Managi, Renewable and Sustainable Energy Reviews **103**,40 (2019).
- [2] N.S.Caetano, T.M.Mata, A.A.Martins, M.C.Felgueiras, Energy Procedia **107**, 7 (2017).
- [3] S.K.Hoekman, A.Broch, X.V.Liu, Renewable and Sustainable Energy Reviews **81**, 3140 (2018).
- [4] O.S.Bushuyev, P.De Luna, C.T.Dinh, L.Tao, G.Saur, J. Van de Lagemaat, E.H.Sargent, Joule **2**(5), 825(2018).
- [5] S.Chu, Y.Cui, N.Liu, Nature materials **16**(1), 16(2017).
- [6] M.Schreier, L.Curvat, F.Giordano, L.Steier, A. Abate, S.M. Zakeeruddin, M.Grätzel, Nature communications **6**(1), 1(2015).
- [7] J.Lin, Z.Pan, X.Wang, ACS Sustainable Chemistry & Engineering **2**(3), 353(2014).
- [8] C.Cometto, R.Kuriki, L.Chen, K.Maeda, T.C.Lau, O.Ishitani, M. Robert, Journal of the American Chemical Society **140**(24), 7437(2018).
- [9] X.Yu, Z.Yang, B.Qiu, S.Guo, P.Yang, B.Yu, Z.Liu, Angewandte Chemie International Edition **58**(2), 632 (2019).
- [10] P.Huang, J.Huang, S.A.Pantovich, A.D.Carl, T.G.Fenton, C.A.Caputo, G. Li, Journal of the American Chemical Society **140**(47), 16042(2018).
- [11] D.Xu, B.Cheng, W.Wang, C.Jiang, J.Yu, Applied Catalysis B: Environmental **231**, 368 (2018).
- [12] C.Yang, Q.Li, Y.Xia, K.Lv, M.Li, Applied Surface Science **464**, 388(2019).
- [13] N.Sadeghi, S.Sharifnia, T.O.Do, T. O, Journal of Materials Chemistry A **6**(37), 18031(2018).
- [14] A.Nakada, T.Nakashima, K.Sekizawa, K. Maeda, O.Ishitani, **7**(7), 4364 (2016).
- [15] S.Guo, H.Zhang, Y.Chen, Z.Liu, B.Yu, Y.Zhao, Z.Liu, ACS Catalysis **8**(5), 4576(2018).
- [16] S.L.Xie, J.Liu, L.Z.Dong, S.L.Li, Y.Q.Lan, Z.M.Su, Chemical science **10** (1),

185 (2019).

- [17] H. Xu, S.Ouyang, L.Liu, P.Reunchan, N. Umezawa, J.Ye, *Journal of Materials Chemistry A***2**(32), 12642 (2014).
- [18] Y.Cao, Q.Li, C.Li, J.Li, J.Yang, J, *Applied Catalysis B: Environmental***198**, 378 (2016).
- [19] X.Meng,S.Ouyang, T.Kako, P.Li, Q.Yu, T.Wang, J.Ye, *Chemical Communications* **50**(78), 11517(2014).
- [20] J.Yu, J.Low, W.Xiao, P.Zhou, M.Jaroniec, *Journal of the American Chemical Society* **136**(25), 8839(2014).
- [21] K. Li, T. Peng, Z. Ying, S. Song, J. Zhang, *Applied Catalysis B: Environmental***180**, 130(2016).
- [22] P. Hu, J.V. Morabito, C.K.Tsung, *ACS Catal.***4**, 4409 (2014).
- [23] F.Vermoortele, A.Vimont, C.Serre, D. de Vos, *Chem. Commun.***47**, 1521 (2011).
- [24] D.Li, S.H.Yu, H.L.Jiang, *Adv. Mater.* **30**, 1 (2018).
- [25] A.Fateeva, P.A.Chater, C.P.Ireland, A.A.Tahir, Y.Z.Khimiya, P.V.Wiper, *Angew. Chem.Int. Ed.* **51**, 7440 (2012).
- [26] X.Chen, Y.Kuwahara, K.Mori, C.Louis, H.Yamashita, *J. Mater. Chem. A* **8**,1904 (2020).
- [27] J.Zhuang, C.H.Kuo, L.Y.Chou, D.Y.Liu, E.Weerapana, C.K.Tsung, *ACS Nano***8**, 2812 (2014).
- [28] F.Ke, Y.P.Yuan, L.G.Qiu, Y.H.Shen, A.J.Xie, J.F.Zhu, X.Y.Tian, L.D.Zhang, *J. Mater. Chem.* **21**, 3843(2011).
- [29] W.Cai, C.C.Chu, G.Liu, Y.X.J.Wáng, *Small***11**, 4806(2015).
- [30] K.D.Nguyen, C.Kutzscher, F.Drache, I.Senkovska, S.Kaskel, *Inorg. Chem.***57**, 1483 (2018).
- [31] C.Wang, M.Zheng, W.Lin, *J. Phys. Chem. Lett.***2**,1701(2011).
- [32] F.Song, C.Wang, W.Lin, *Chem. Commun.* **47**, 8256 (2011).
- [33] H.C.Zhou, J.R.Long, O.M.Yaghi, *Chem. Rev.***112**, 673(2012).
- [34] A. Khutia, Ch. Janiak, *Dalton Trans.* **43**, 1338(2014).
- [35] J. A. Botas, G. Calleja, M. Sanchez-Sanchez, M.G. Orcajo, *Langmuir***26**, 5300 (2010).
- [36] S. N. Kim, S. T. Yang, J. Kim, J. E. Park, W.S. Ahn, *CrystEngComm*, **14**, 4142 (2014).
- [37] Y. Le, D. Guo, B. Cheng and J. Yu, *J. Colloid Interface Sci.* **408**, 173 (2013).
- [38] Y. S. Bae, R. Q. Snurr, *Angew. Chem., Int. Ed.* **50**, 11586 (2011).
- [39] K. Lee, J. D. Howe, L. Ch. Lin, B. Smit, J. B. Neaton, *Chem. Mater.* **27**, 668(2015).
- [40] P.Verma, Y.Kuwahara, K.Mori, H.Yamashita, *J. Mater. Chem. A***4**, 10142 (2016).
- [41] F.Guo, S.Yang, Y.Liu, P.Wang, J.Huang, W.Y.Sun, *ACS Catal.***9**, 8464(2019).
- [42] L.Chen, Y.Wang, F.Yu, X.Shen, C.Duan, *J. Mater. Chem.***A7**, 11355(2019).
- [43] F.Guo, Y.P.Wei, S.Q.Wang, X.Y.Zhang, F.M.Wang, W.Y.Sun, *J. Mater. Chem. A***7**, 26490 (2019).
- [44]B.Han, X.Ou, Z.Deng, Y.Song, C.Tian, H.Deng, Y.J.Xu, Z.Lin, *Angew. Chem. Int. Ed.* **57**, 16811(2018).
- [45] H.Jiang, S.Gong, S.Xu, P.Shi, J.Fan, V.Cecen, Q.Xu, Y.Min, *Dalt. Trans.* **49**, 5074(2020).
- [46] M.Chen, L.Han, J.Zhou, C.Sun, C.Hu, X. Wang, Z.Su, *Nanotechnology***29**, 284003(2018).
- [47] F. Guo, S. Yang, Y.Liu, P.Wang, J.Huang, W.Y.Sun, *ACS Catal.* **9**, 8464 (2019).
- [48] J.Xu, X.Liu, Z.Zhou, M. Xu *Appl. Surf. Sci.***513**, 145801(2020).
- [49] Y.F.Xu, M.Z.Yang, B.X.Chen, X.D.Wang, H.Y. Chen, D. B. Kuang, *J. Am. Chem.Soc.* **139**, 5660 (2017).
- [50] L.Zhao, Z.Zhao, Y.Li, X.Chu, Z.Li, Y.Qu, L.Bai, L.Jing, *Nanoscale* **12**, 10010 (2020).
- [51] G. Ferey, C. Mellot-Draznieks, C. Serre, F. Millange, J. Dutour, S. Surble, I. Margiolaki, *Science***309**, 2040 (2005).
- [52] Z. Saedi, Sh. Tangestaninejad, M. Moghadam, V. Mirkhani, I. Mohammadpour-Baltork, *Catal. Commun.* **17**, 18 (2012).
- [53] M. Sánchez-Sánchez, N. Getachew, K. Díaz, M. Díaz-García, Y. Chebude, I. Díaz, *Green Chem.***17**,1500 (2015).
- [54] T. Grant Glover, G.W. Peterson, B.J. Schindler, D. Britt, O. Yaghi, *Chem. Eng. Sci.***66**,

163(2011).

[55] A. Wang, Y. Zhou, Z. Wang, M. Chen, L. Sunc, X. Liu, RSC Adv. **6**, 3671(2016).

[56] H.Hu, X. Lou, C.Li, X. Hu, T.Li, Q.Chen, M.Shen, B.Hu, New J Chem **40**,9746 (2016).

[57] R. BoopathiRaja, M. Parthibavarman, J. Alloy. Compd. **811**, 152084(2019).

[58] N.Sasirekha, S.J.S.Basha, K.Shanth, App. Catal. B-Environ. **62**(1), 169 (2006).

[59] K.Koči, L.Obalova, L.Matějova, D.Placha,, Z.Lacny, J.Jirkovsky, O.Šolcova, App. Catal. B-Environ. **89**(3), 494(2009).

[60] P.SivaKarthik, V. Thangaraj, S. Kumaresan, K. Vallalperuman,Journal of Materials Science: Materials in Electronics **28**(14),10582 (2017).

[61] V. Binas, D.Venieri, D. Kotzias, G.Kiriakidis, J. Materiomics **3**(1), 3 (2017).

[62] L.Mao, K.Ye, X.Li, J.Zhang, T.Liu, L.Peng, Zan, Appl. Catal. B Environ. **144**, 855(2014).